

The Angular Momentum of Gas in Proto-Galaxies: II – The Impact of Preheating

Frank C. van den Bosch¹, Tom Abel², and Lars Hernquist³ \star

¹*Max-Planck-Institut für Astrophysik, Karl Schwarzschild Str. 1, 85741 Garching, Germany*

²*The Pennsylvania State University, University Park, PA 16802, USA*

³*Harvard Smithsonian Center for Astrophysics, Cambridge, MA 02138 USA*

ABSTRACT

We examine the effect of preheating of the intergalactic medium on galaxy formation using cosmological hydrodynamical simulations. By performing simulations both with and without a simple model for preheating, we analyse and compare the angular momentum distributions of the dark matter and the baryons. Preheating unbinds baryons from their dark matter haloes, yielding a baryonic mass fraction that declines with decreasing halo mass. In addition, the spin parameter of the gas is reduced with respect to the case without preheating, while the misalignment between the angular momentum directions of the gas and dark matter increases strongly. The angular momentum distributions of individual haloes reveal that preheating decreases (increases) the mass fraction with low (negative) specific angular momentum. We discuss the implications of these findings for the formation of disk galaxies in a preheated intergalactic medium, and compare our results to the predictions of Maller & Dekel (2002), who propose an alternative interpretation for the origin of the angular momentum of (proto)-galaxies.

Key words: cosmology: dark matter — galaxies: formation — galaxies: structure — galaxies: haloes.

1 INTRODUCTION

Angular momentum plays a crucial role in the formation and structuring of galaxies. This is most evident for disk galaxies, whose structure and dynamics are clearly governed by their angular momentum content. In current models for disk galaxy formation, set forth by White & Rees (1978) and Fall & Efstathiou (1980), it is supposed that a disk forms out of gas that cools inside a dark matter halo while conserving its specific angular momentum acquired from cosmological torques. Under the additional assumption that the gas and dark matter acquire the same quantities of specific angular momentum (generally expressed through the dimensionless spin parameter λ), this model can successfully explain the observed distribution of disk scale-lengths (e.g., Mo, Mao & White 1998; de Jong & Lacey 2000).

Nevertheless, a proper understanding of the structure and formation of disk galaxies in terms of the origin and evolution of their angular momentum distributions has proved extremely challenging. Foremost, hydrodynamical simulations of disk formation that include cooling indicate that, contrary to the standard assumption, the specific angular momentum distribution of the gas is *not* conserved. Instead,

the gas loses a large fraction of its angular momentum to the dark matter (Navarro & Benz 1991; Navarro & White 1994), yielding disks that are an order of magnitude too small. This problem has become known as the “angular momentum catastrophe”, and is typically associated with the well-known “over-cooling problem” in CDM cosmologies (White & Rees 1978; White & Frenk 1991). At early-times gas cooling is very efficient, leading to the formation of dense gas clumps which lose their orbital angular momentum to the surrounding dark matter haloes through dynamical friction, before eventually merging to form the central disk. Therefore, some mechanism is required to prevent or delay the cooling of the gas, so that it can preserve a larger fraction of its angular momentum. Indeed, simulations in which gas cooling is artificially suppressed until $z = 1$ yield larger, more realistic disks (Weil, Eke & Efstathiou 1998; Eke, Efstathiou & Wright 2000).

The outstanding challenge is to identify what mechanism can accomplish this required delay, and yet be consistent with observations of galaxies and quasars at high redshift. Initial studies focussed on heating from the extragalactic ionising background. Although these studies have shown that an ionising background can have a non-negligible impact on the formation of (mainly small) galaxies, the impact on the angular momenta of disk galaxies was found to be ei-

\star E-mail: vdbosch@mpa-garching.mpg.de

ther unimportant (Vedel, Hellsten & Sommer-Larsen 1994) or exacerbated the problem (Navarro & Steinmetz 1997).

More promising results have been obtained with localised feedback from supernova explosions. Simulations that model this type of feedback typically reveal a significantly reduced, though not entirely nullified, angular momentum loss (Sommer-Larsen et al. 1999; Sommer-Larsen, Götz & Portinari 2002; Thacker & Couchman 2000, 2001). However, the implications of these results are still somewhat unclear, in view of the difficulty of modeling the physical properties of star-forming gas in a cosmological context. In their recent study of cosmic star formation (Springel & Hernquist 2003a), Springel & Hernquist (2003b) developed a multiphase description of the interstellar medium and showed that one consequence of feedback is to pressurise the gas, altering its equation of state at high densities. Their idealised models of disk formation in dark matter haloes indicate that this process is highly sensitive to the form of the equation of state of star-forming gas, which may help to reconcile the earlier simulations with observations.

Furthermore, pressure forces associated with galactic winds may significantly affect the baryonic mass fractions (Scannapieco, Ferrara & Broadhurst 2000) and/or angular momenta (Abel, Croft & Hernquist 2001) of neighbouring proto-galaxies, making the impact less localised than typically assumed. A related form of feedback is preheating (or rather ‘reheating’) of the intergalactic medium (IGM) during an early epoch of vigorous star formation and/or AGN activity. Characteristic of preheating is that the entropy of the IGM is increased substantially before the main epoch of galaxy formation; i.e. before the majority of the gas has undergone gravitational collapse. This can significantly delay cooling (i.e., Mo & Mao 2002) and therefore alleviate the angular momentum catastrophe (Sommer-Larsen et al. 1999).

However, even if feedback can prevent the angular momentum catastrophe, an important discrepancy between the angular momenta of dark matter haloes and disk galaxies remains. If the standard picture is correct, the angular momentum distribution of disk galaxies should be identical to that of dark matter haloes. However, the universal angular momentum distribution of dark matter haloes (Bullock et al. 2001), contains far more low-angular momentum material than is typically present in disk galaxies (van den Bosch 2001; van den Bosch, Burkert & Swaters 2001). In a recent paper, Maller & Dekel (2002; hereafter MD02) proposed a toy model which indicates that the same feedback that may solve the angular momentum catastrophe can also explain this apparent mismatch of angular momentum profiles. Although angular momentum is commonly thought to arise from cosmological torques (Hoyle 1953; Peebles 1969; White 1984), the MD02 model is based on an alternate, though related picture put forward by Vitvitska et al. (2002) and Maller, Dekel & Somerville (2002), in which the final angular momentum of a dark matter halo is simply the vector sum of the orbital angular momenta of all its progenitor haloes. In this model, most of a halo’s final angular momentum owes to the last major merger, while the low-angular momentum material originates from the many small satellites accreted from largely uncorrelated directions. If, within this picture, low mass galaxies are largely devoid of baryonic material (because of feedback processes), the angular momentum of the final disk material may have a substantially

smaller fraction of low angular momentum material than the corresponding dark matter halo. This would explain the deficit of low angular momentum material in observed dwarf galaxies, and, according to MD02, may even result in systems in which the baryons have a larger spin parameter than the dark matter.

In an ongoing attempt to improve our understanding of the origin and evolution of the angular momentum of baryons, we have performed a number of simulations of structure formation in a Λ CDM cosmology *without cooling*. While unrealistic, the absence of cooling allows us to better focus attention on the impact of gravity and (shock) heating on the angular momentum of the baryons. Therefore, such simulations are a logical preliminary step to investigate the build-up of angular momentum in proto-galaxies. In the first paper in this series (van den Bosch et al. 2002; hereafter Paper I), we used a non-radiative[†], hydrodynamic N -body simulation to investigate whether the gas and dark matter acquire identical angular momentum distributions. Although this is the general assumption, based on the fact that the gas and dark matter experience the same cosmological torques, gas and dark matter suffer different relaxation mechanisms during halo collapse. Whereas the dark matter undergoes collisionless virialisation through violent relaxation, gas achieves hydrostatic equilibrium by shocking. In principle, this could decouple the angular momentum distribution of the gas from that of the dark matter, possibly explaining the mismatch of angular momentum profiles discussed above without the need for feedback. However, we found that the “initial” (i.e., prior to cooling) angular momentum distributions of gas and dark matter are remarkably similar. This indicates that shock heating does not lead to a decoupling of the angular momenta of gas and dark matter and it thus confirms one of the two main assumptions underlying the theory of disk galaxy formation. However, we found that the angular momentum *directions* of the gas and dark matter are poorly aligned, and that large mass fractions of the gas (and dark matter) have negative specific angular momentum with respect to the total angular momentum vector (see also Chen & Jing 2002). This indicates that disk galaxy formation *cannot* occur under detailed angular momentum conservation, in violation of the second main assumption underlying the theory of disk galaxy formation.

Yoshida et al. (2003) also report a misalignment between gas and dark matter total angular momenta at high redshifts in simulations with 2×288^3 particles and in volumes 600 comoving kpc on a side. The pressure forces in their calculations stem from the inherent IGM pressure relevant at the low mass scales of first structure formation. Their very high resolution calculation validates our conclusions of Paper I and illustrates the importance of pressure forces for the angular momentum properties of gas with respect to dark matter.

In this paper we present a similar simulation as in Paper I, but this time include a model for preheating. We analyse the angular momentum distributions of the gas and dark matter, which we compare to one another and to results

[†] We use the term “non-radiative”, rather than the commonly used term “adiabatic”, to emphasise that the simulation does include non-adiabatic shocks.

without preheating. The main goals of this paper are: (i) to investigate the impact of preheating on the angular momentum of the baryons (again in the limit without cooling), and (ii) to test various predictions of the MD02 model.

This paper is organised as follows. In Section 3 we describe the numerical simulations and the analysis. Section 2 presents the results, and discusses the implications for the formation of disk galaxies in a preheated intergalactic medium. Finally, we summarise our findings in Section 5.

2 THE IMPACT OF PREHEATING

Preheating of the intergalactic medium was originally introduced to explain the observed X-ray properties of clusters of galaxies (Evrard & Henry 1991; Kaiser 1991) and is still considered one of the most likely explanations for the observed L_X - T relation of groups and clusters of galaxies (e.g., Balogh, Babul & Patton 1999; Bower et al. 2001; Tozzi & Norman 2001; Borgani et al. 2002; Tornatore et al. 2003). Preheating also has a number of effects on the formation of galaxies. Foremost, due to the pressure increase, baryons can unbind themselves from their dark matter haloes, an effect that is larger for less massive haloes. In addition, the hot gas in hydrostatic equilibrium inside dark matter haloes has much shallower density distributions than without preheating, which causes cooling to be more gradual and more simultaneous (Mo & Mao 2002). This (partially) decouples the gas from the hierarchical, bottom-up structure formation, which may explain why the colour-magnitude relations of galaxies are “inverted” with respect to simple, hierarchical expectations (Kauffmann, White & Guiderdoni 1993; Baugh, Cole & Frenk 1996; Cole et al. 2000; van den Bosch 2002). A potential problem, however, is that too much preheating, or at a too early stage, can delay star-formation to unrealistically low redshifts (Tornatore et al. 2002). Preheating has also been advocated as a means to alleviate the X-ray halo problem (White & Frenk 1991; Pen 1999; Benson et al. 2000). However, detailed simulations by Toft et al. (2002) indicate that simple cooling flow models overpredict X-ray luminosities and that no X-ray halo problem exists. Furthermore, the work by Tornatore et al. (2002) indicates that, contrary to naive expectations, preheating can actually *increase* the X-ray emissivity.

Preheating is also expected to impact on the angular momentum of (proto)-galaxies. First of all, since preheating alleviates the overcooling problem, it is to be expected that it also helps in reducing/solving the angular momentum catastrophe. Second, preheating increases the internal pressure of the gas, which causes the *baryonic* proto-galaxy during the pre-collapse era to be larger (which tends to increase the angular momentum because it enlarges the torquing arm) and more spherical (which tends to lower the angular momentum because the moment of inertia is reduced). Finally, after collapse and virialisation, only a small fraction of the baryons have remained bound to the system. Since the outer parts (which become unbound) typically contain most of the high angular momentum material, this reduction of the baryonic mass fraction is most likely associated with a reduction of the total specific angular momentum. Furthermore, if the MD02 picture for angular momentum acquisition is correct, preheating might result in lower mass

fractions of low angular momentum material because low mass satellites will have lower baryonic mass fractions than their more massive counterparts. The main goal of this paper is to establish which of these various effects dominates, and to investigate in detail what the final outcome of preheating is on the angular momentum content of the baryons.

Despite the large number of studies related to preheating, the actual energy source responsible for the heating is highly speculative. Some constraints can be placed however. First of all, the observed presence of the Ly α forest indicates that preheating can not have occurred uniformly over the entire IGM. This rules exotic preheating-candidates, such as decaying dark matter, unlikely. Furthermore, if preheating is mainly due to Type II supernovae, the IGM would be enriched to oxygen-abundances that are only consistent with observations in the central parts of nearby galaxy clusters (see discussion in Sommer-Larsen et al. 1999). Since, at early times, vigorous star formation (and AGN activity) occurs predominantly in (proto)-groups and clusters, this may simply be another argument for a certain amount of non-uniformity in the preheating. Despite these constraints, until the energy source is known and understood, the epoch, amount, and (non)-uniformity of preheating are largely to be considered free model parameters.

3 NUMERICAL SIMULATION

To illustrate the effects of preheating on the angular momentum of the gas in proto-galaxies, we perform the same numerical simulation as described in Paper I, but modified to include the effects of preheating. The simulation computes the evolution of an initial Gaussian random field of dark matter particles and non-radiative baryons in a Λ CDM cosmology with $\Omega_m = 0.3$, $\Omega_\Lambda = 0.7$ and with a baryon density of $\Omega_b = 0.021h^{-2}$ with $h = H_0/(100 \text{ km s}^{-1} \text{ Mpc}^{-1}) = 0.67$. We use the smoothed particle hydrodynamics (SPH) code GADGET (Springel, Yoshida & White 2001) to evolve the density field inside a box of $10h^{-1} \text{ Mpc}$ (comoving) from redshift $z = 59$ down to $z = 3$. The initial density field is realised adopting identical power-spectra for baryons and dark matter normalised to $\sigma_8 = 0.9$. We use 128^3 (2.1 million) gas and dark matter particles each, with particle masses of $m_{\text{gas}} = 6.26 \times 10^6 h^{-1} M_\odot$ and $m_{\text{DM}} = 3.34 \times 10^7 h^{-1} M_\odot$, respectively. The gravitational softening lengths for both the gas and the dark matter are 4 kpc (comoving). All results presented below correspond to the final output at $z = 3$.

The gas has an initial entropy corresponding to a temperature of $2 \times 10^4 \text{ K}$ for a mean molecular weight of one proton mass. At redshift $z = 7$ we reset the temperature of the gas particles to $4 \times 10^6 \text{ K}$ (again for a mean molecular weight of one proton mass) to mimic the effects of preheating. Although this is a fairly ad-hoc method, especially in terms of the abruptness and spatial uniformity of the preheating, it is adequate to illustrate the type of changes that preheating may have on the final angular momentum distribution of the gas in galaxy sized haloes. To place the *magnitude* of this preheating model in a broader context, we follow Mo & Mao (2002), and define the entropy of the gas as $\mathcal{S} = T/n_e^{2/3}$, with T the temperature and n_e the electron density (assuming a completely ionised gas). For a cosmology with $\Omega_b = 0.021h^{-2}$ and $h = 0.67$, as adopted here, the

entropy in units of 100 keV cm^{-2} at an overdensity δ and a redshift z can be written as

$$S_{100} = \left(\frac{T}{4 \times 10^4 \text{ K}} \right) (1 + \delta)^{-2/3} (1 + z)^{-2} \quad (1)$$

(Mo & Mao 2002). Thus, a temperature of $T = 4 \times 10^6 \text{ K}$ at $z = 7$ corresponds to $S_{100} = 1.6(1 + \delta)^{-2/3}$, which is comparable to the observed entropy excess in clusters and groups (Ponman, Cannon & Navarro 1999; Lloyd-Davies, Ponman & Cannon 2000), and does not violate constraints from the CMB (e.g. Springel et al. 2001). Note that the simulation does not include radiative cooling, and that we can thus not investigate whether preheating indeed helps to solve the angular momentum catastrophe (but see Sommer-Larsen et al. 1999).

3.1 Halo Identification

As detailed in Paper I, groups of particles are identified with the HOP group finder (Eisenstein & Hut 1998). In each group we identify the densest particle, and we determine the virial radius R_{vir} of the spherical volume, centered on this densest particle, inside of which the average dark matter density is $\Delta_{\text{vir}}(z)$ times the critical density $\rho_{\text{crit}}(z)$. For our adopted cosmology and at the redshift of the output analysed $\Delta_{\text{vir}} = 174.7$ (Bryan & Norman 1998). Next, we compute the center-of-mass of all dark matter particles inside this spherical volume which we associate with the new center of the halo. We compute the new R_{vir} around this new halo center, as well as the associated new center-of-mass. This procedure is iterated until the distance between the center-of-mass and the adopted halo center is less than one percent of the virial radius R_{vir} . Typically, this requires of order 2 to 5 iteration steps.

All dark matter and gas particles inside the resulting spherical volume with radius R_{vir} are considered halo members. Although our iterative method ensures that the center-of-mass of the dark matter component is similar to the adopted halo center, the same is not necessarily true for the gas component. We therefore remove all haloes from our sample for which the distance between the halo center and the center-of-mass of the gas particles is larger than 10 percent of R_{vir} (see Paper I for details). In addition, if any two haloes overlap, i.e., if the distance between the halo centers is less than the sum of their virial radii, we remove the least massive halo from our sample. In order to allow sufficiently accurate measurements of the angular momentum vectors of the gas and dark matter, we accept only haloes that have more than 100 gas particles *and* more than 100 dark matter particles. This leaves a total of (only) 68 haloes. For comparison, in the simulation without preheating described and analysed in Paper I, we obtained a sample of 378 haloes (using exactly the same halo identification and sample selection). The reason why so far fewer haloes make it into the sample with preheating is that the average number of gas particles per halo is significantly reduced (see below).

3.2 Analysis

Spin parameters and mis-alignment angles between gas and dark matter components are computed in the standard way,

as described in detail in Paper I. The spin parameters of the dark matter and the gas are defined by

$$\lambda_{\text{gas,DM}} = \frac{|\mathbf{j}_{\text{gas,DM}}|}{\sqrt{2} R_{\text{vir}} V_{\text{vir}}}, \quad (2)$$

where \mathbf{j}_{gas} and \mathbf{j}_{DM} are the specific angular momenta of the gas and dark matter, respectively, and $V_{\text{vir}} = \sqrt{G(M_{\text{gas}} + M_{\text{DM}})/R_{\text{vir}}}$ is the circular velocity at the virial radius R_{vir} . The angle between the angular momentum vectors of both mass components is defined as

$$\theta = \cos^{-1} \left[\frac{\mathbf{J}_{\text{gas}} \cdot \mathbf{J}_{\text{DM}}}{|\mathbf{J}_{\text{gas}}| |\mathbf{J}_{\text{DM}}|} \right], \quad (3)$$

with \mathbf{J}_{gas} and \mathbf{J}_{DM} being the total angular momentum vectors of the gas and dark matter, respectively.

Following Paper I, for haloes with more than 5000 particles (in total) we compute the detailed distributions of specific angular momenta of the gas and DM particles. Both the dark matter and the gas are fluids, for which the velocity of each *microscopic* particle can be written as $\mathbf{v} = \mathbf{u} + \mathbf{w}$. Here \mathbf{u} is the mean streaming motion at the location \mathbf{x} of the microscopic particle, and \mathbf{w} is the particle's random motion. The velocities of the DM particles in the simulation correspond to \mathbf{v} and are obtained from Newton's equations of motion. In the case of the gas, however, the SPH approach is used, which yields the streaming motions \mathbf{u} of the gas particles by solving the Euler equations (with some artificial viscosity to take account of shocks). Information about the random motion of the gas particles is provided by the internal energy of each particle.

Thus, the velocities of the dark matter particles and gas particles in the simulation correspond to different motions. To compare the angular momentum distributions of the gas and dark matter in a meaningful way, however, the same velocities have to be used. Ideally, one would focus on the angular momentum distributions based on the streaming motions $\mathbf{u}(\mathbf{x})$. After all, when the gas cools $\mathbf{v} \rightarrow \mathbf{u}$, i.e., the typical random motions become negligible. Under the assumption that the gas conserves its specific angular momentum, the resulting disk will thus have an angular momentum distribution related to \mathbf{u} . However, this requires estimating the streaming motions of the dark matter. In principle this could be achieved by smoothing the dark matter velocities \mathbf{v} , but it is unclear what smoothing scale to use and resolution issues are likely to play an important role. We therefore do not attempt to compute the dark matter streaming motions, but instead use the velocities \mathbf{v} of the dark matter and gas particles when comparing their angular momentum distributions. To compute the microscopic velocities \mathbf{v} of the gas particles, we use the same 'thermal broadening' technique as described in Paper I. For each gas particle we draw 100 random velocities \mathbf{w} which we add to the particle's streaming motion \mathbf{u} . For each of the three Cartesian components of \mathbf{w} we draw a velocity from a Gaussian with a standard deviation given by

$$\sigma = \sqrt{\frac{kT}{\mu}} = \sqrt{\frac{2U}{3}} \quad (4)$$

Here U and T are the internal energy per unit mass and temperature of the gas particle, respectively, k is Boltzmann's constant, and μ is the mean molecular weight of the gas. For each particle (gas and dark matter) we compute the compo-

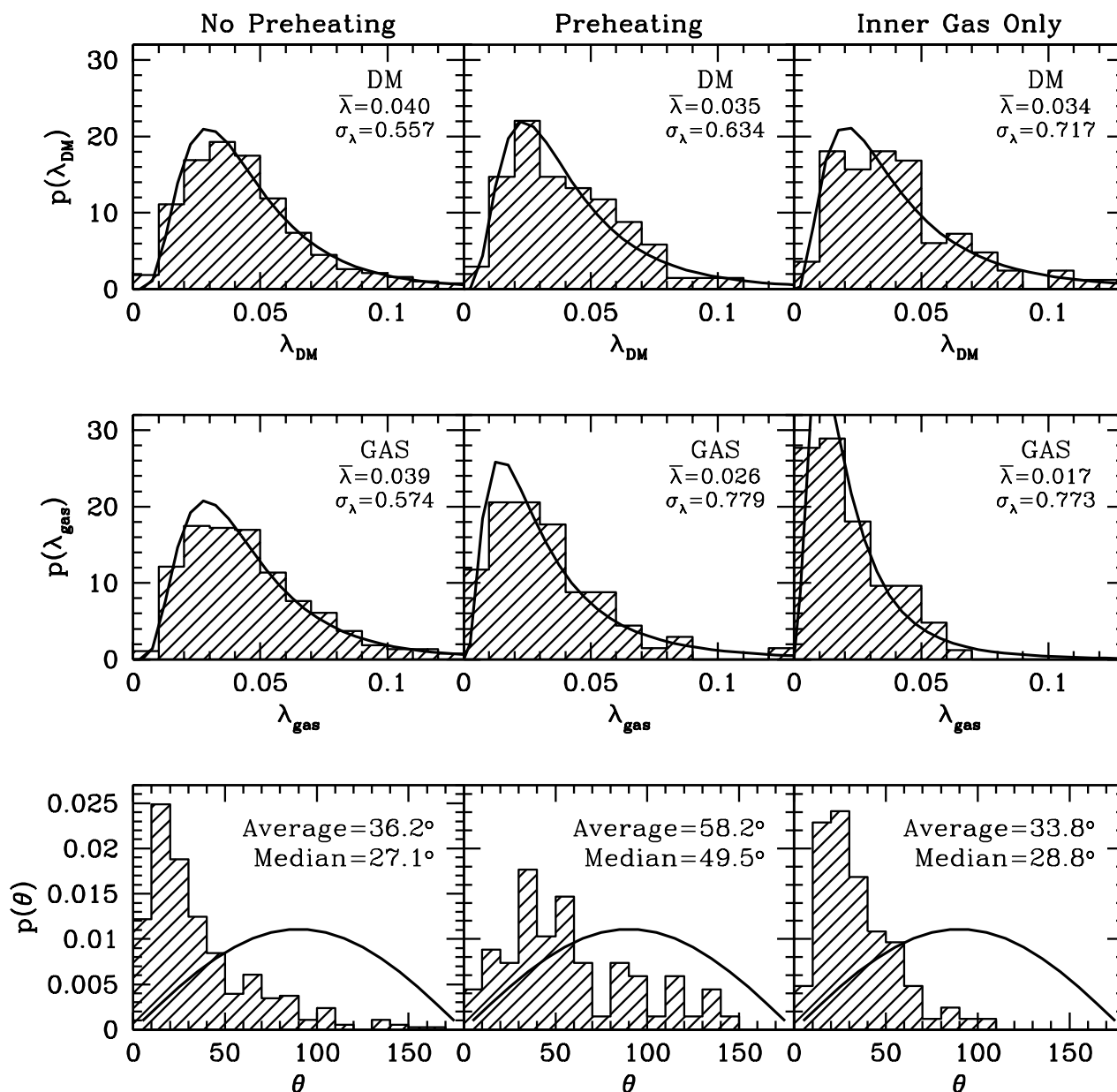


Figure 2. Distributions of λ_{DM} (upper panels), λ_{gas} (middle panels), and the misalignment angle between the angular momentum vector of the gas and the dark matter, θ (lower panels). Results are shown for haloes in the simulation without (left-hand panels) and with (middle column) preheating. In addition, we show the results for the “inner gas only” sample of haloes (right-hand panels) extracted from the no-preheating simulation as described in the text. The solid lines in the upper and middle panels correspond to the best-fit log-normal distributions (eq. [6]), with the best-fit values of $\bar{\lambda}$ and σ_λ as indicated. The solid line in the lower panels correspond to a random distribution of angles, and is shown for comparison. See text for a detailed discussion of the results.

ment j^v of the specific angular momentum $\mathbf{j}^v = \mathbf{r} \times \mathbf{v}$ that is aligned with the *total* angular momentum vector \mathbf{J} . We use the superscript v to distinguish it from the specific angular momentum $\mathbf{j} = \mathbf{r} \times \mathbf{u}$, which is only accessible for the baryons.

4 RESULTS

4.1 Baryonic mass fractions

Fig. 1 plots the baryonic mass fraction $M_{\text{gas}}/M_{\text{vir}}$ as a function of halo virial mass $M_{\text{vir}} = M_{\text{gas}} + M_{\text{DM}}$. Results are shown for the case with (tripods) and without (triangles) preheating. Whereas the baryonic mass fractions in haloes without preheating are close to the universal value $f_{\text{bar}} = \Omega_b/\Omega_m$ (indicated by horizontal, dotted line), in the preheating simulation the gas mass within the virial radii of dark matter haloes is significantly suppressed. This sup-

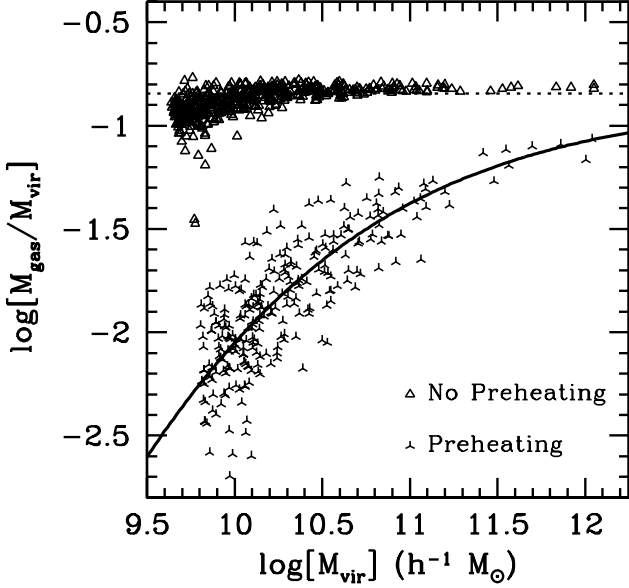


Figure 1. Baryonic mass fractions, $M_{\text{gas}}/M_{\text{vir}}$, as function of halo virial mass, M_{vir} , for the haloes in the simulations without (triangles) and with (tripods) preheating. The horizontal, dotted line corresponds to the universal baryon fraction $f_{\text{bar}} = \Omega_b/\Omega_m$. In the no-preheating simulation the baryonic mass fractions of all haloes are very similar to this universal value. In the preheating case, however, gas mass fractions are systematically lower, an effect that is larger for lower mass haloes. The thick solid line is the best-fit relation of the form (5).

pression is larger for smaller mass haloes and can be parameterised using the fitting formula suggested by Gnedin (2000):

$$M_{\text{gas}} = \frac{f_{\text{bar}} M_{\text{DM}}}{\left[1 + (2^{\alpha/3} - 1) \left(\frac{M_f}{M_{\text{DM}}}\right)^\alpha\right]^{3/\alpha}} \quad (5)$$

Here α and the filter mass M_f are free fitting parameters. Our best-fit relation is shown as a thick solid line in Fig. 1 and has $\alpha = 0.4$ and $M_f = 5 \times 10^{11} h^{-1} M_\odot$.

We can use this fitting function to gain some insight in how preheating affects the angular momentum distribution of the baryons. We reanalyse the no-preheating simulation presented in Paper I, but this time considering only the inner-most gas mass fraction whose mass is given by equation (5) with $\alpha = 0.4$ and $M_f = 5 \times 10^{11} h^{-1} M_\odot$. Applying the same halo selection criteria as described in Section 3.1 we end up with 83 haloes, which we analyse exactly as before. In what follows, we refer to this sample of haloes as the “inner gas only” sample. If the differences between the no-preheating and preheating simulations are predominantly due to the fact that in the latter only the most bound fraction of the gas remains within the virial radius, this “inner gas only” sample should reveal similar angular momentum distributions as in the preheating simulation.

4.2 Spin parameters & misalignment angles

In Fig. 2, we compare the spin parameter distributions of the gas and dark matter, and contrast the simulations with and without preheating. The hatched histograms in the up-

per, middle, and lower panels plot the distributions of the spin parameter of the dark matter, $p(\lambda_{\text{DM}})$, of the spin parameter of the gas, $p(\lambda_{\text{gas}})$, and of the angle between the angular momentum vectors of both mass components, $p(\theta)$, respectively. Panels on the left correspond to the simulation without preheating (cf., Paper I), panels in the middle correspond to the simulation with preheating, and panels on the right correspond to the simulation without preheating, but in which only the inner fraction of the gas is used in the analysis (as described above). The thick solid lines in the upper and middle panels indicate the best-fit log-normal distributions

$$p(\lambda)d\lambda = \frac{1}{\sqrt{2\pi}\sigma_\lambda} \exp\left(-\frac{\ln^2(\lambda/\bar{\lambda})}{2\sigma_\lambda^2}\right) \frac{d\lambda}{\lambda}. \quad (6)$$

with the best-fit values of $\bar{\lambda}$ and σ_λ indicated. The thick solid lines in the lower panels correspond to a random distribution of angles θ , and are shown for comparison.

As already discussed in Paper I, the spin parameter distributions of the gas and dark matter are remarkably similar in the case without preheating. However, in the preheating simulation presented here, there is a clear indication that $\lambda_{\text{gas}} < \lambda_{\text{DM}}$ on average. For the dark matter $\bar{\lambda}_{\text{DM}} = 0.035$ and $\sigma_{\lambda_{\text{DM}}} = 0.63$ (almost identical to the no-preheating case), while for the gas $\lambda_{\text{gas}} = 0.025$ and $\sigma_{\lambda_{\text{gas}}} = 0.76$. Preheating has reduced the typical specific angular momentum of the gas with respect to that of the dark matter and with respect to that of the gas in the no-preheating case. In addition, with an average (median) of 58.2° (49.5°) the θ -distribution in the case with preheating is clearly different from the case without preheating. Although it is still significantly different from that of a purely random distribution, preheating has largely decoupled the angular momentum directions of the gas and dark matter.

If the differences between the no-preheating and preheating simulations result predominantly from the fact that in the latter case only the most bound fraction of the gas ends up inside the virial radius, the haloes of the “inner gas only” sample should reveal similar distributions of λ_{gas} and θ as for those with preheating. This, however, is clearly not the case: $p(\lambda_{\text{gas}})$ is shifted to even lower values, while the distribution of θ is virtually indistinguishable from that of the no-preheating simulation (and thus differs strongly when preheating is included). The increase in the misalignment found in the preheating simulation is thus not merely due to the fact that only the inner fraction of the gas remains bound to the halo. Apparently preheating has modified the inertia tensor of the gas with respect to that of the dark matter, which has resulted in a larger average misalignment between the two mass components. In addition, this comparison indicates that the fraction that remains bound in the case with preheating has acquired *more* specific angular momentum as the same mass in the case without preheating. This is due to the fact that the extent (and thus the torquing arm) of that gas is larger in the case of preheating, and/or, to differences in the relative importance of low mass progenitors, as suggested by MD02.

4.3 Angular Momentum Distributions

In the previous section we compared the distributions of the (global) spin parameters of dark matter and gas, both

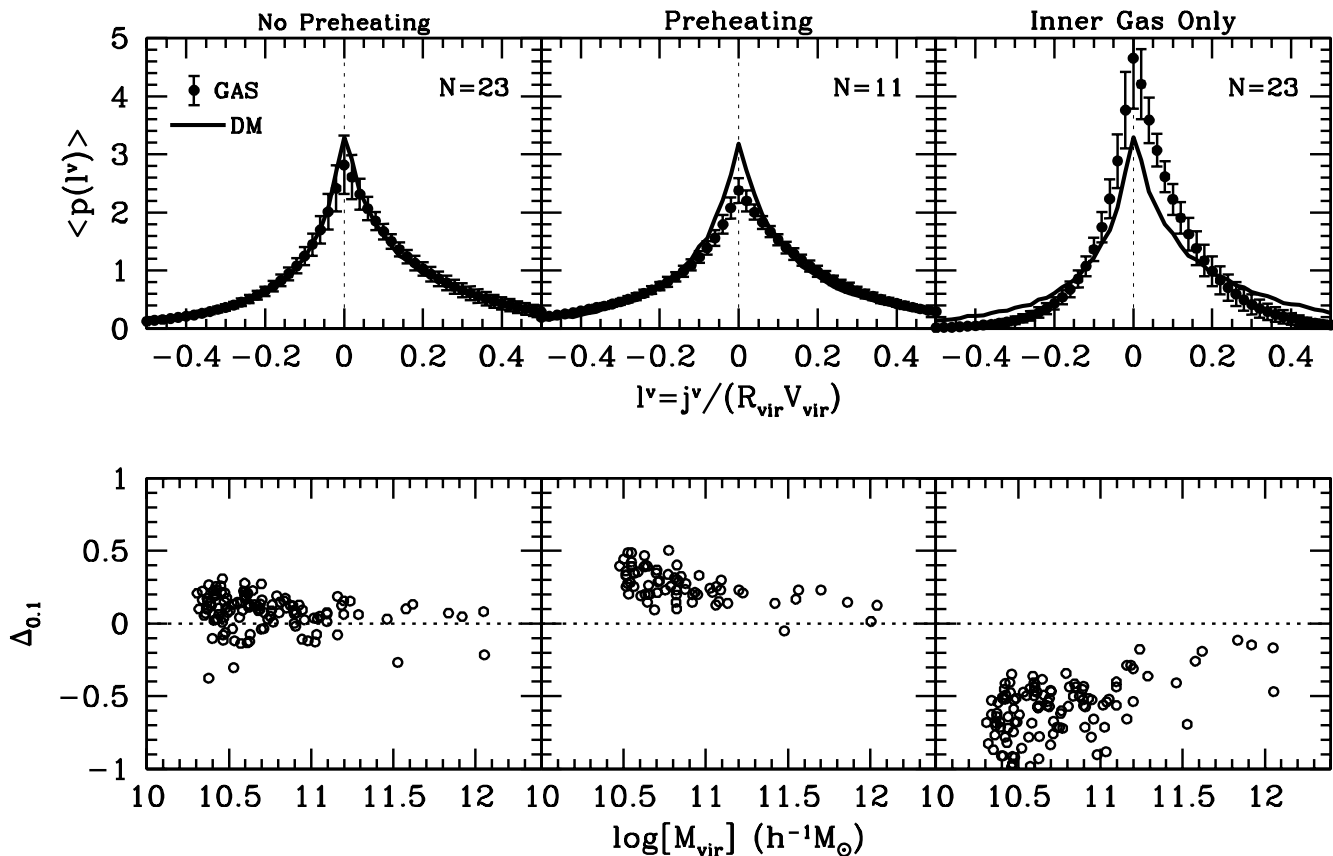


Figure 3. Upper panels plot the distribution of normalised, specific angular momentum, l^v , averaged over all haloes (the actual number, N , is indicated in each panel) with more than 5000 particles in total. Results are shown for three samples of haloes, as indicated above each panel. Solid lines and dots with errorbars (corresponding to the rms scatter) correspond to the angular momentum distributions of the dark matter and gas, respectively. Whereas the $\langle p(l^v) \rangle$ of the gas and dark matter are indistinguishable in the case without preheating, the gas lacks predominantly low angular momentum material with respect to the dark matter in the simulation with preheating. The opposite is true for the inner gas mass fraction in haloes without preheating (right-hand panel). These results are confirmed in the lower panels, which plot $\Delta_{0.1}$ (equation [8]) as function of halo virial mass. The quantity $\Delta_{0.1}$ is a measure for the difference between the mass fractions of dark matter and gas with $|l^v| < 0.1$. In the no-preheating simulation, $\Delta_{0.1} \sim 0$ independent of halo mass. With preheating, however, $\Delta_{0.1}$ decreases with decreasing halo mass, consistent with the predictions of Maller & Dekel (2002). The “inner gas only” sample reveals the opposite behaviour, indicating that low angular momentum material resides predominantly near the center of the potential well.

with and without preheating. Here, we compare the angular momentum distributions within individual haloes.

As described in Section 3.2, for each particle we compute the specific angular momentum j^v along the direction of the total angular momentum vector. Following Paper I we define the normalised specific angular momenta $l^v = j^v / (R_{\text{vir}} V_{\text{vir}})$ and compute separate, normalised distribution functions $p(l^v)$ for the gas and dark matter in each individual halo. Because of this normalisation, the distributions of different haloes can be compared directly, and be used to compute the *average* distribution function

$$\langle p(l^v) \rangle = \frac{1}{N} \sum_{i=1}^N p_i(l^v) \quad (7)$$

where the average is taken over the N haloes with more than 5000 particles in total. In the simulation without preheating there are $N = 23$ haloes that make our selection criterion, which is reduced to $N = 11$ in the case with preheating. The upper panels of Fig. 3 plot $\langle p(l^v) \rangle$ for both the dark

matter (solid line) and the gas (solid dots). The errorbars correspond to the rms of the scatter about the mean, and, for clarity, are only plotted for the gas.

The upper left panel of Fig. 3, which corresponds to the simulation without preheating, confirms the conclusion from Paper I that the angular momentum distributions of the gas and dark matter are virtually identical, and thus that the shocks that occur during virialisation do not significantly modify the angular momentum distribution of the gas. The upper middle panel, which corresponds to the simulation with preheating, however, shows a clear deficit of low angular momentum material for the gas with respect to that of the dark matter. This is in good agreement with predictions from the MD02 model, even though the effect shown is fairly small. However, this may be due to the fact that we have included only massive haloes with more than 5000 particles, while MD02 predict that the effect is stronger in less massive haloes. In order to investigate this mass dependence and to make the differences between $p(l^v_{\text{gas}})$ and $p(l^v_{\text{DM}})$ at low l^v more quantitative, we define the statistic

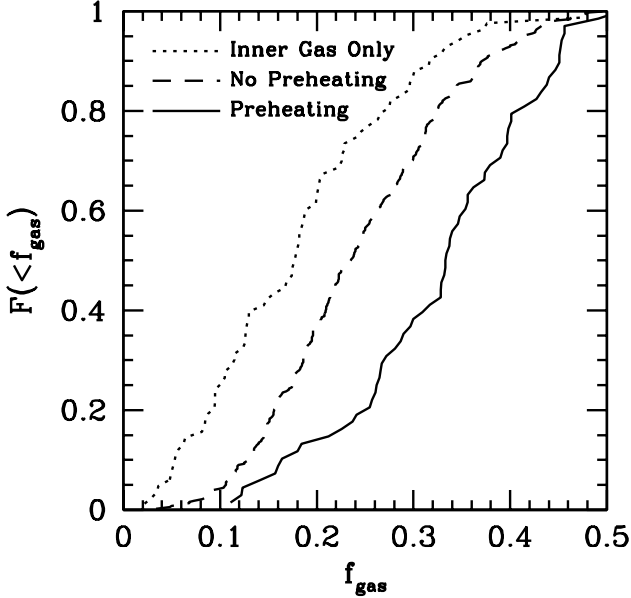


Figure 4. Cumulative distributions of the baryonic mass fractions with $j < 0$ (with j determined from the actual *streaming* motion of the gas). Results are shown for the “preheating” ($N = 68$), the “no-preheating” ($N = 378$) and the “inner gas only” ($N = 83$) samples, as indicated. Simple K-S tests indicate that all three distributions are very significantly different from one-another. Note that the “preheating” case reveals the distribution that is most skewed towards relatively large mass fractions with negative specific angular momentum. Apparently, preheating causes an increase in f_{gas} and thus in the decoherence of the streaming motions of the gas.

$$\Delta_{0.1} = 1 - \frac{\int_{-0.1}^{0.1} p(l_{\text{gas}}^v) dl_{\text{gas}}^v}{\int_{-0.1}^{0.1} p(l_{\text{DM}}^v) dl_{\text{DM}}^v} \quad (8)$$

which is a measure of the difference between the dark matter and baryonic mass fractions with $|l^v| \leq 0.1$. The lower panels of Fig. 3 plot $\Delta_{0.1}$ as function of virial mass. In order to increase the number statistics we have included all haloes with more than 1000 particles in total. Whereas $\Delta_{0.1} \sim 0$, independent of halo mass, in the case without preheating, there is a clear trend of decreasing $\Delta_{0.1}$ with decreasing halo mass in the case with preheating. This indicates that lower mass haloes contain relatively smaller baryonic mass fractions with low angular momentum, in excellent agreement with the MD02 model.

The right-hand panels of Fig. 3 show $\langle p(l^v) \rangle$ and $\Delta_{0.1}(M_{\text{vir}})$ for the “inner gas only” sample. Here, the baryonic material clearly has much *more* low angular momentum material than the dark matter. In addition, this effect becomes stronger for lower mass haloes. A comparison with the preheating results clearly proves that preheating has not merely “stripped” the outer layers of gas from the dark matter haloes, but has also affected the actual angular momentum distribution of the remaining gas.

In addition to the mass fraction of low angular momentum material, another useful statistic regarding the angular momentum distributions are the fractions f_{DM}^v and f_{gas}^v of dark matter and gas particles, respectively, that have *negative* specific angular momentum. Note that negative here means that the angle ϕ between the total angular momen-

tum vector and the particle’s angular momentum vector $\mathbf{j}^v = \mathbf{r} \times \mathbf{v}$ lies in the range $90^\circ < \phi \leq 180^\circ$. As shown in Paper I, f^v is anti-correlated with the spin parameter, such that systems with higher specific angular momentum have lower mass fractions with $j^v < 0$. As can be seen from the average distributions $\langle p(l^v) \rangle$ shown in the upper panels of Fig. 3 the average mass fraction with $j^v < 0$ is fairly large (~ 40 percent). This, however, is to a large extent a reflection of the fact that the random motions \mathbf{w} are larger than the streaming motions \mathbf{u} . As indicated in Section 3.2 (see also Paper I), the more illustrative angular momentum distribution is the one based on the streaming motions, $p(l)$. Here $l = j/(R_{\text{vir}}V_{\text{vir}})$ with j the component of the specific angular momentum vector $\mathbf{j} = \mathbf{r} \times \mathbf{u}$ that is aligned with the total angular momentum vector \mathbf{J} . As shown in Paper I, $p(l)$ typically has a less extended wing to negative specific angular momentum than $p(l^v)$ and a more pronounced peak at low angular momentum.

Fig. 4 plots the *cumulative* distributions of the baryonic mass fractions, f_{gas} , with $l < 0$. Results are shown for all three samples and take all haloes with more than 100 gas particles and more than 100 dark matter particles into account. Although the median of these distributions is clearly smaller than the ~ 0.4 in the case of f_{gas}^v , they indicate a significant amount of decoherence in the streaming motions of the gas. As detailed in Paper I, this implies that disk formation cannot occur under detailed conservation of specific angular momentum, posing new challenges to the usual picture of disk formation. In the “inner gas only” case, the distribution of f_{gas} is shifted slightly to lower values compared to the no-preheating case. The K-S test indicates a probability of 10^{-5} that both are drawn from the same distribution. This indicates that the amount of decoherence is radially dependent, in agreement with the notion that material accreted at different times introduces a radial dependence of the angular momentum direction (Ryden 1988; Quinn & Binney 1992). In the case *with* preheating, the median of $p(f_{\text{gas}})$ is *larger* than in the case without preheating. According to the K-S test, the probability that both $p(f_{\text{gas}})$ are drawn from the same parent distribution is only 9.8×10^{-9} . This indicates that preheating significantly increases the mass fraction with negative specific angular momentum.

5 DISCUSSION & CONCLUSIONS

A full understanding of the structure and formation of disk galaxies within a hierarchical, cold dark matter cosmogony faces a number of intriguing challenges. First, in the absence of any heating, baryons cool extremely efficiently, producing too many satellite galaxies and resulting in what has become known as the angular momentum catastrophe. In addition, the angular momentum distributions of both the gas and the dark matter in numerical simulations reveal an excess of low angular momentum material compared to real disk galaxies. Moreover, as shown by van den Bosch et al. (2002), virialised systems reveal large mass fractions with *negative* specific angular momentum. Since disks typically contain no negative specific angular momentum material, disk formation cannot occur under detailed conservation of specific angular momentum, contrary to standard assumptions.

It is generally hoped that these problems subside when

feedback related heating effects are included. Arguably, the most popular feedback effect is heating of the cold gas in galaxies by the energy feedback from star formation. In semi-analytical models for galaxy formation this type of feedback is typically implemented in such a way that large fractions of the cold gas are ejected from the galaxy and/or the dark matter halo. Although these “galactic winds” may successfully explain several of the observed properties of galaxies, it remains unclear whether this picture is realistic. For instance, detailed hydrodynamical simulations have shown that the actual mass ejection efficiencies may be much smaller than typically assumed (Mac Low & Ferrara 1999; Strickland & Stevens 2000).

The preheating investigated in this paper is an alternative form of feedback which relies on heating the gas before it becomes part of a virialised dark matter halo. This type of feedback has mainly been discussed in connection with the observed entropy excess in groups and clusters of galaxies (e.g., Kaiser 1991; Ponman et al. 1999; Borgani et al. 2002), but might be of equal importance for galaxy formation (Mo & Mao 2002). However, unlike the supernova-induced feedback mentioned above, the energy source for preheating is highly speculative. Possible candidates include high-redshift (starburst) galaxies, population III stars, active galactic nuclei, or even the decay of some dark matter species. Therefore, until the energy source is known and understood, the epoch and (non)-uniformity of preheating are to be considered free model parameters (see Section 2 for a more detailed discussion).

In this paper we investigated the impact of preheating on the angular momentum of gas in proto-galaxies. To that end, we used a numerical simulation of structure formation in a standard Λ CDM cosmology with non-radiative gas, in which we mimic an extreme form of preheating by instantaneously and homogeneously increasing the temperature of the gas at $z = 7$. Although somewhat unrealistic, the amount of entropy injected into the gas is consistent with the observed entropy excess in groups and clusters of galaxies. By comparing the angular momentum distributions of gas and dark matter both in simulations with and without preheating we identified the following effects;

- preheating unbinds baryons from dark matter haloes, resulting in a baryonic mass fraction that decreases with decreasing halo mass.
- with preheating, the spin parameter of the gas within the virial radius is smaller than that of all gas within the virial radius in the case without preheating, but larger than that of the inner most gas with the same mass.
- preheating largely decouples the angular momentum directions of the gas and dark matter.
- preheating decreases the baryonic mass fractions with low specific angular momentum.
- preheating increases the baryonic mass fractions with negative specific angular momentum.

These effects are most easily understood by considering that preheating increases the internal pressure of the gas. This means that the gas associated with a proto-galaxy becomes more extended, and more spherical in shape. Part of the gas can become unbound, which explains the reduced baryonic mass fractions. In addition, this partially explains why the spin parameter of the gas that remains bound to

the dark matter haloes is reduced. The baryons that have become unbound were mostly located at larger radii, which experience the largest torquing forces. Thus, the unbinding preferentially removes the high angular momentum material. In addition, the internal pressure of the gas modifies the moment of inertia with respect to that of the underlying dark matter, which explains why the directions of the angular momentum vectors of the gas and the dark matter are so strongly decoupled. The reduction in the mass fraction with low angular momentum may be understood as due to the modification of the density profile of the gas due to the increased internal pressure. As shown by Mo & Mao (2002), preheating creates extremely shallow density distributions for the gas. This means that there is relatively less material with a small moment of inertia, and thus a reduction in the fraction of low angular momentum material.

The above interpretation is based on the standard idea that the angular momentum results from cosmological torques acting on a proto-galaxies with a non-zero moment of inertia. However, in recent papers Vitvitska et al. (2002) and Maller et al. (2002) have proposed an alternative model, in which the angular momentum is due to the orbital angular momentum from the progenitors. Maller & Dekel (2002) have presented a toy-model based on this picture that includes the effects of feedback. They argue that as long as feedback effects imply a baryonic mass fraction that declines with decreasing halo mass (as is the case for the preheating model presented here), the gas in the final halo should have: (i) a spin parameter that is typically larger than that of its dark matter halo, and (ii) an angular momentum distribution with relatively less low angular momentum material. Our results disagree with (i), but confirm (ii), including the prediction that the effect should be stronger for less massive haloes. At first sight it may seem contradictory that we find a reduction of the mass fraction with low angular momentum, yet a decrease in the total angular momentum. The explanation, however, is that the mass fraction with negative specific angular momentum has increased, which has a stronger impact on λ_{gas} than the reduction of low angular momentum material.

The origin of this increase in the mass fraction with negative specific angular momentum is not clear, neither in the MD02 scenario nor in the cosmological torque picture. In principle, the *presence* of negative specific angular momentum is more easily understood in terms of the satellite accretion model. However, there is no obvious explanation for why the amount of negative specific angular momentum should increase in a preheated IGM. Note that we have focused on the simplest possible form of the role of pressure forces namely uniform preheating at high redshifts. Our particular finding that preheating increases the baryonic mass fractions with negative specific angular momentum may change as one considers different forms of feedback. For example, winds produced by galaxies with high star formation rates are likely to produce complex flow patterns around them, as illustrated by figures 5-8 in Springel & Hernquist (2003b). The pressure forces arising from such winds will act differently than the ones caused by our preheating scheme. Studying these more subtle differences in feedback prescriptions will require a large suit of higher resolution numerical simulations that are beyond the scope of the present investigation.

Our results have important implications for the formation of disk galaxies. As we have shown, preheating can regulate the baryonic mass fractions of dark matter haloes in much the same way as galactic winds, and should therefore be able to alleviate the angular momentum catastrophe. Indeed, simulations by Sommer-Larsen et al. (1999) that include both cooling and preheating find a reduction (although modest) of the angular momentum loss of the baryons. Furthermore, the reduction of the baryonic mass fraction with low angular momentum material is advantageous for the formation of realistic disks. However, preheating also has some effects that are less favourable for disk formation. First of all, the total specific angular momentum of the gas within the virial radius, and which is thus eligible to cool and form a disk galaxy, is reduced with respect to that of the dark matter. Thus, although the angular momentum loss may be reduced, there is less angular momentum to start with. Second, the detailed angular momentum distributions reveal a clear increase of the baryonic mass fractions with negative specific angular momentum, making the formation of a disk dominated galaxy less plausible. We therefore conclude that understanding disk formation remains an intriguing puzzle, even in a preheated IGM.

ACKNOWLEDGEMENTS

We thank Houjun Mo and Simon White for stimulating discussions, and the referee, Jesper Sommer-Larsen, for his comments that helped improve the presentation of the paper. This work was supported in part through NSF grants ACI96-19019, AST-9803137, AST 99-00877, and AST 00-71019. and through the Grand Challenge Cosmology Consortium.

REFERENCES

- Abel T., Croft R.C., Hernquist L., 2001, preprint (astro-ph/0111046)
- Balogh M.L., Babul A., Patton D.R., 1999, MNRAS, 307, 463
- Baugh C.M., Cole S., Frenk C.S., 1996, MNRAS, 283, 1361
- Benson A.J., Bower R.G., Frenk C.S., White S.D.M., 2000, MNRAS, 314, 557
- Borgani S., Governato F., Wadsley J., Menci N., Tozzi P., Quinn T., Stadel J., Lake G., 2002, MNRAS, 336, 409
- Bower R.G., Benson A.J., Lacey C.G., Baugh C.M., Cole S., Frenk C.S., 2001, MNRAS, 325, 497
- Bryan G., Norman M., 1998, ApJ, 495, 80
- Bullock J.S., Dekel A., Kolatt T.S., Kravtsov A.V., Klypin A.A., Porciani C., Primack J.R., 2001, ApJ, 555, 240
- Chen D.N., Jing Y.P., 2002, MNRAS, 336, 55
- Cole S., Lacey C.G., Baugh C.M., Frenk C.S., 2000, MNRAS, 319, 168
- de Jong R.S., Lacey C., 2000, ApJ, 545, 781
- Eisenstein D.J., Hut P., 1998, ApJ, 496, 605
- Eke V.R., Efstathiou G., Wright L., 2000, MNRAS, 315, L18
- Evrard A.E., Henry J.P., 1991, ApJ, 383, 95
- Fall S.M., Efstathiou, G., 1980, MNRAS, 193, 189
- Gnedin N.Y., 2000, ApJ, 542, 535
- Hoyle F., 1953, ApJ, 118, 513
- Kaiser N., 1991, ApJ, 383, 104
- Kauffmann G., White S.D.M., Guiderdoni B., 1993, MNRAS, 264, 201
- Lloyd-Davies E.J., Ponman T.J., Cannon D.B., 2000, MNRAS, 315, 689
- Mac Low M.M., Ferrara A., 1999, ApJ, 513, 142
- Maller A.H., Dekel A., 2002, MNRAS, 335, 487 (MD02)
- Maller A.H., Dekel A., Somerville R., 2002, MNRAS, 329, 423
- Mo H.J., Mao S., White S.D.M., 1998, MNRAS, 295, 319
- Mo H.J., Mao S., 2002, MNRAS, 333, 768
- Navarro J.F., Benz W., 1991, ApJ, 380, 320
- Navarro J.F., White S.D.M., 1994, MNRAS, 267, 401
- Navarro J.F., Steinmetz M., 1997, ApJ, 478, 13
- Peebles P.J.E., 1969, ApJ, 155, 393
- Pen U.-L., 1999, ApJ, 510, L1
- Ponman T.J., Cannon D.B., Navarro J.F., 1999, Nature, 397, 135
- Quinn T., Binney J.J., 1992, MNRAS, 255, 729
- Ryden B.S., 1988, ApJ, 329, 589
- Scannapieco E., Ferrara A., Broadhurst T., 2000, ApJ, 536, L11
- Sommer-Larsen J., Gelato S., Vedel H., 1999, ApJ, 519, 501
- Sommer-Larsen J., Götz M., Portinari L., 2002, preprint (astro-ph/0204366)
- Springel V., Yoshida N., White S.D.M., 2001, New Astronomy, 6, 79
- Springel V., Hernquist L., 2003a, MNRAS, 339, 312
- Springel V., Hernquist L., 2003b, MNRAS, 339, 289
- Springel V., White, M., Hernquist L., 2001, ApJ, 549, 681
- Strickland D.K., Stevens I.R., 2000, MNRAS, 314, 511
- Thacker R.J., Couchman H.M.P., 2000, ApJ, 545, 728
- Thacker R.J., Couchman H.M.P., 2001, ApJ, 555, L17
- Toft S., Rasmussen J., Sommer-Larsen J., Pedersen K., 2002, MNRAS, 335, 799
- Tornatore L., Borgani S., Springel V., Matteucci F., Menci N., Murante G., 2003, preprint (astro-ph/0302575)
- Tozzi P., Norman C., 2001, ApJ, 546, 63
- van den Bosch F.C., 2001, MNRAS, 327, 1334
- van den Bosch F.C., 2002, MNRAS, 332, 456
- van den Bosch F.C., Burkert A., Swaters R.A., 2001, MNRAS, 326, 1205
- van den Bosch F.C., Abel T., Croft R.A.C., Hernquist L., White S.D.M., 2002, ApJ, 576, 21 (Paper I)
- Vedel H., Hellsten U., Sommer-Larsen J., 1994, MNRAS, 271, 743
- Vitvitska M., Klypin A.A., Kravtsov A.V., Wechsler R.H., Primack J.R., Bullock J.S., 2002, ApJ, 581, 799
- Weil M.L., Eke V.R., Efstathiou G., 1998, MNRAS, 300, 773
- White S.D.M., 1984, MNRAS, 286, 38
- White S.D.M., Rees M.J., 1978, MNRAS, 183, 341
- White S.D.M., Frenk C.S., 1991, ApJ, 379, 52
- Yoshida N., Abel T., Hernquist L., Sugiyama N., 2003, ApJ, preprint (astro-ph/0301645)